Mitochondria as signaling organelles in the vascular endothelium

Marisol Quintero*, Sergio L. Colombo*, Andrew Godfrey, and Salvador Moncada†

Wolfson Institute for Biomedical Research, University College London, Cruciform Building, Gower Street, London WC1E 6AE, United Kingdom

Contributed by Salvador Moncada, February 8, 2006

Vascular endothelial cells are highly glycolytic and consume relatively low amounts of oxygen (O_2) compared with other cells. We have confirmed that oxidative phosphorylation is not the main source of ATP generation in these cells. We also show that at a low O_2 concentration (<1%) endogenous NO plays a key role in preventing the accumulation of the α-subunit of hypoxia-inducible factor 1. At higher O_2 concentrations (1–3%) NO facilitates the production of mitochondrial reactive oxygen species. This production activates the AMP-activated protein kinase by a mechanism independent of nucleotide concentrations. Thus, the primary role of mitochondria in vascular endothelial cells may not be to generate ATP but, under the control of NO, to act as signaling organelles using either O_2 or O_2-derived species as signaling molecules. Diversion of O_2 away from endothelial cell mitochondria by NO might also facilitate oxygenation of vascular smooth muscle cells.

AMP-activated protein kinase | hypoxia-inducible factor 1α | hypoxia | nitric oxide

Endogenously synthesized nitric oxide (NO) is a highly diffusible gas that has a variety of physiological functions, some of which are mediated by activation of the soluble guanylate cyclase enzyme (1). In the last decade cytochrome *c* oxidase, the terminal enzyme in the mitochondrial electron transport chain, has also been identified as a target of the action of NO (2–4). Acting on the latter enzyme, NO can regulate cellular oxygen (O_2) consumption (5) and the mitochondrial redox state, facilitating the release of free radicals, which act as a signaling mechanism (6). Furthermore, inhibition of mitochondrial O_2 consumption by NO leads to a situation in which, though O_2 might be available, cells and tissues are unable to use it. This phenomenon has been termed "metabolic hypoxia," a condition that differs from true hypoxia in which O_2 availability is insufficient (5). In metabolic hypoxia there is also a redistribution of O_2 away from mitochondria toward nonrespiratory O_2-dependent targets (7). Inhibition of cell respiration by NO is also known to activate glycolysis in some cells through a mechanism involving activation of 6-phosphofructo-2-kinase (8).

Although we have previously demonstrated that endogenous NO regulates O_2 consumption in vascular endothelial cells and other cell types ($RAW_{246.7}$) (6, 9), the consequences of this effect have yet to be studied in detail. Of particular interest are the consequences in vascular endothelial cells, which have been known for some time to be glycolytic (10) and to possess high concentrations of constitutive NO (9).

To investigate the bioenergetic and signaling consequences of the action of NO on cytochrome *c* oxidase in vascular endothelial cells, we have studied the behavior of two key transduction mechanisms involved in the response to hypoxia and in the regulation of the bioenergetic status of the cell, namely hypoxia-inducible factor 1 (HIF-1) (11–13) and AMP-activated protein kinase (AMPK) (14, 15). Our results suggest that, in human endothelial cells, mitochondria under the control of NO regulate the activity of both HIF-1 and AMPK in a manner consistent with a role as signaling organelles, independent of their bioenergetic functions.

Results

Contribution of Mitochondrial Respiration and Glycolysis to the Generation of ATP in Human Umbilical Vein Endothelial Cells (HUVECs). The role of mitochondrial O_2 consumption on ATP production in HUVECs was investigated by measuring ATP concentrations ([ATP]) after exposing the cells to different O_2 concentrations (21%, 3%, 1.5%, and <0.5%) for up to 2 h. Table 1 shows a small (≈25%) but significant decrease in [ATP] when the O_2 concentration was 1.5% or below. The use of pharmacological electron transport chain inhibitors such as rotenone or antimycin at ambient O_2 concentration had similar effects, causing an ATP reduction of ≈30%. No further reduction in [ATP] was seen when electron transport chain-inhibited cells were incubated at a lower O_2 concentration (i.e., <0.5%). Pretreatment of the cells with an inhibitor of the glycolytic pathway [20 mM 2-deoxy-D-glucose (2DG)] led to a greater decrease in the intracellular [ATP] (≈50%) at any O_2 concentration studied. The AMP:ATP ratio from cells exposed to 3% O_2 was not significantly different from those at 21% O_2 (Table 2). However, a significant increase (≈2-fold) in the AMP:ATP ratio was observed after incubation of HUVECs with 2DG; this increase was even greater (6- to 7-fold) when 2DG was combined with rotenone.

NO Prevents the Accumulation of HIF-1α at Low Oxygen Concentrations. To investigate the effect of constitutively generated NO on the stabilization of HIF-1α by low O_2 concentration, we exposed HUVECs to a variety of O_2 concentrations (21%, 6%, 3%, 1.5%, and 0.5%) in the presence or absence of the NO synthase inhibitor N^G-monomethyl-L-arginine (L-NMMA). Unlike other human cells [smooth muscle cells and human epithelial kidney cells (HEK293)], no significant accumulation of HIF-1α was observed in HUVECs until the O_2 concentration was reduced to 0.5% O_2 (Fig. 1*A*). Treatment of HUVECs with L-NMMA led to HIF-1α stabilization at a higher O_2 concentration compared with control cells (Fig. 1*A*) but did not affect the O_2 concentration at which nonendothelial cells stabilize HIF-1α (data not shown). Human microvascular endothelial cells, which also generate NO from endothelial NO synthase (eNOS) (16), responded in a similar manner to HUVECs when they were exposed to low O_2 concentrations in the absence or presence of the NOS inhibitor (Fig. 1*B*). In cells that were pretreated with the inhibitor of mitochondrial respiration myxothiazol, however, L-NMMA did not affect HIF-1α stabilization at 1.5% O_2, indicating that inhibition of the electron transport chain (and subsequent redistribution of O_2) was responsible for the observed destabilization of HIF-1α (Fig. 1*C*). Studies on DNA binding in nuclear extracts confirmed the activation of HIF-1

Conflict of interest statement: No conflicts declared.

Abbreviations: AMPK, AMP-activated protein kinase; HIF-1, hypoxia-inducible factor 1; HUVEC, human umbilical vein endothelial cell; DHE, dihydroethidine; eNOS, endothelial NO synthase; ROS, reactive oxygen species; L-NMMA, N^G-monomethyl-L-arginine; 2DG, 2-deoxy-D-glucose.

*M.Q. and S.L.C. contributed equally to this work.

†To whom correspondence should be addressed. E-mail: s.moncada@ucl.ac.uk.

CELL BIOLOGY

Table 1. Bioenergetic assessment in HUVECs

	ATP nmol/10^6 cells				
$[O_2]$	Control	2DG	Rotenone	Antimycin	2DG plus rotenone
21%	11.3 ± 1.1	5.7 ± 0.9**	9.6 ± 1.0**	7.3 ± 0.5**	0.6 ± 0.1**
3%	9.3 ± 1.7	5.3 ± 1.0**	7.2 ± 1.4**	7.8 ± 1.5	0.8 ± 0.3**
1.5%	9.1 ± 0.6*	4.2 ± 0.2**	9.3 ± 1.1	7.2 ± 1.3**	0.6 ± 0.3**
<0.5%	8.3 ± 1.2*	2.9 ± 0.4**	8.5 ± 1.1	7.7 ± 0.7	0.4 ± 0.1**

Effects of glycolytic and mitochondrial inhibitors on [ATP], at different O_2 concentrations. Treatments were carried out for 2 h at the indicated O_2 concentration before [ATP] was determined by chemiluminescence. For details of procedures, see *Materials and Methods.* Data represent the mean ± SEM of at least four independent experiments. 2DG, 20 mM; rotenone, 0.5 μM, antimycin, 0.5 μM. *, Significantly different from control at 21% ($P < 0.05$); **, significantly different from respective control ($P < 0.05$).

(Fig. 1*D*). To investigate whether the observed effect of L-NMMA was due to inhibition of NO production, eNOS expression in endothelial cells was blocked by using RNA interference methodology. Western blot analysis of eNOS short-hairpin RNA-infected cells showed a reduction (80%) of eNOS expression (Fig. 1*E*) and HIF-1α stabilization at a higher O_2 concentration (i.e., 1.5%) compared with mock-infected cells (0.5%) (Fig. 1*F*).

Reactive Oxygen Species (ROS) Generation Depends on Oxygen Concentrations. The production of superoxide ($O_2^{\bullet-}$) was studied in HUVECs incubated in the presence or absence of antioxidants (50 μM MnTBAP plus 1 mM ascorbic acid) at different O_2 concentrations. Fig. 2*A* shows representative confocal images of the cells after incubation with dihydroethidine (DHE) at 21% and 3% O_2. Fig. 2*B* summarizes the quantitative analysis of DHE oxidation product measurements. No significant difference was observed in the fluorescence of cells incubated at 21% in the presence or absence of antioxidants. When cells were incubated at 3% O_2, however, there was a significant increase in the fluorescence of control cells, which was prevented by antioxidants (6.38 ± 0.73 vs. 3.41 ± 1.01 arbitrary units for control and antioxidant-treated cells, respectively). To address the role of NO in the generation of ROS observed at 3% O_2, HUVECs were incubated with and without L-NMMA at 21% and 3% O_2. Inhibition of NO synthesis abolished the increase in the fluorescence observed at 3%, but it did not affect the fluorescence at 21% (Fig. 2*B*). Cells incubated at 0.5% O_2 did not show an increase in fluorescence.

AMPK Activation Depends on O_2 Concentration. When tested at different O_2 concentrations, the activation of AMPK was found to be undetectable at 21% O_2, to be maximal at 3% O_2, and to decrease at lower O_2 concentrations (Fig. 3*A*). Activation at 3% O_2, however, did not appear to be mediated by AMP, because the AMP:ATP ratio was not different from that observed under normoxic conditions (Table 2). Moreover, AMP levels did not seem to increase even when O_2 concentrations were reduced further, despite the fact that under these conditions a small decrease in ATP was evident (compare Table 2 with Table 1). In contrast, at 21% O_2, treatment with the glycolytic inhibitor 2DG, alone or together with a mitochondrial inhibitor, increased the AMP:ATP ratio substantially (Table 2) and activated AMPK (Fig. 3*B*).

Table 2. AMP:ATP ratios in HUVECs

	AMP:ATP ratio		
$[O_2]$	CTRL	2DG	2DG plus rotenone
21%	0.095 ± 0.010	0.187 ± 0.009*	0.664 ± 0.012**
3%	0.091 ± 0.024	0.176 ± 0.017*	0.557 ± 0.055**
1.5%	0.127 ± 0.007	0.291 ± 0.013**	1.007 ± 0.148**
<0.5%	0.116 ± 0.030	0.362 ± 0.029*	1.157 ± 0.172**

Effects of glycolytic and ETC inhibitors on AMP:ATP ratios at different O_2 concentrations. Treatments were carried out for 2 h before samples were processed. Each individual sample was neutralized, centrifuged, and filtered before HPLC separation. For further details of procedures, see *Materials and Methods.* Data represent the mean ± SEM of at least three independent experiments. 2DG, 20 mM; rotenone, 0.5 μM. *, Significantly different from control ($P < 0.05$); **, significantly different from control ($P < 0.01$).

ROS-Dependent AMPK Activation at Low O_2 Concentration in HUVECs. The contribution of ROS to AMPK activation was investigated by treatment of HUVECs with different prooxidant regimens. Fig. 4*A* shows that incubation of HUVECs with *tert*-butylhydroxyperoxide led to the phosphorylation of AMPK at 21% O_2. Similarly, exposure of HUVECs to angiotensin II, which is known to activate NADPH oxidase (17), resulted in AMPK activation in a dose-dependent manner (Fig. 4*B*). Based on these results, we investigated whether the observed activation of AMPK at 3% O_2 was due to the ability of HUVECs to generate ROS under these conditions. As shown in Fig. 5*A*, the presence of antioxidants (MnTBAP plus ascorbic acid) led to a decrease in the amount of phosphorylated AMPK (pAMPK) in HUVECs exposed to 3% O_2. Similar results were observed with ρ^0 cells, which lack functional mitochondria (Fig. 5*B*).

Discussion

We have found that endothelial cells from various origins, including microvascular endothelium, stabilize HIF-1α at a lower O_2 concentration than other cells. Indeed, whereas human epithelial kidney and smooth muscle cells stabilize this transcription factor at 3% O_2, the endothelial cell does this only at <1% O_2. Our experiments suggest that this observation, which has been described previously but not remarked on (18, 19), may be attributed, at least in part, to NO acting on the mitochondrion to divert O_2 away from it toward the cytosol; this diversion maintains the activation of the prolyl hydroxylases as we have reported before (7). This hypothesis is supported by the observation that treating HUVECs with L-NMMA to inhibit NO generation or silencing eNOS both lead to an increase in the O_2 concentration at which HIF-1α is stabilized, i.e., to 1.5%. Furthermore, this effect of L-NMMA is not observed in cells that have previously been treated with myxothiazol to inhibit their mitochondrial O_2 consumption, thus adding support to the contention that HIF-1α destabilization by NO occurs as a consequence of the redistribution of O_2 to the prolyl hydroxylases.

A ROS-dependent mechanism has been suggested to play a role in HIF-1α stabilization in hypoxia in different cell types (20). This does not seem to be the case in HUVECs, where our

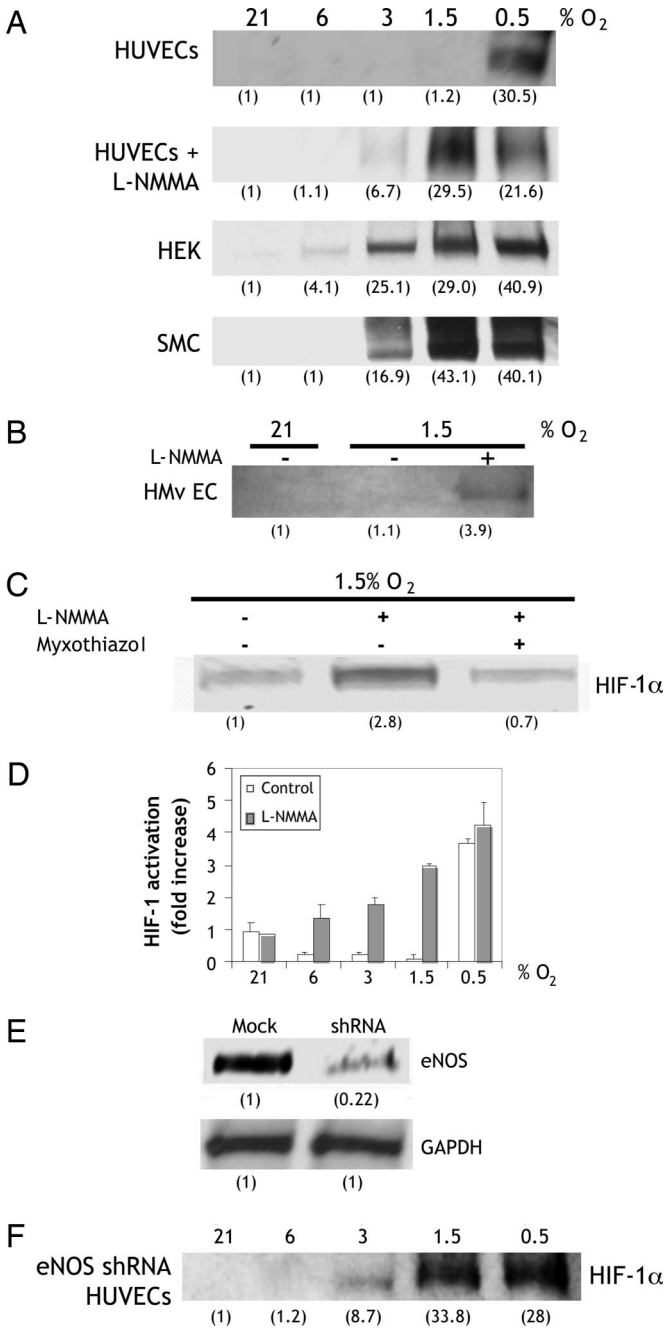

Fig. 1. Effect of endogenous NO on HIF-1α accumulation at different O_2 concentrations. HIF-1α protein levels were detected by Western blotting of nuclear extracts from HUVECs, HEK293 cells, and smooth muscle cells (*A*) or human microvascular endothelial cells (*B*) exposed for 8 h to the indicated O_2 concentration in the absence or presence of L-NMMA (1 mM). (*C*) HIF-1α protein levels from nuclear extract of HUVECs exposed to 1.5% O_2 in the presence or absence of L-NMMA and myxothiazol. (*D*) HIF-1α DNA-binding activity in nuclear extracts from HUVECs exposed to O_2 concentration as in *A*. The values represent the mean ± SEM from three independent experiments. (*E*) HUVECs infected with short-hairpin RNA eNOS exhibited markedly reduced eNOS expression levels after 2 weeks when compared with wild-type cells. GAPDH was used as protein loading control. (*F*) HIF-1α protein levels from nuclear extract of silenced eNOS cells exposed to different O_2 concentrations. Values in brackets are the estimations from densitometry analysis.

results show that the highest release of ROS occurs at an O_2 concentration around 3%. At this point we did not observe maximal HIF-1α stabilization; however, we did observe

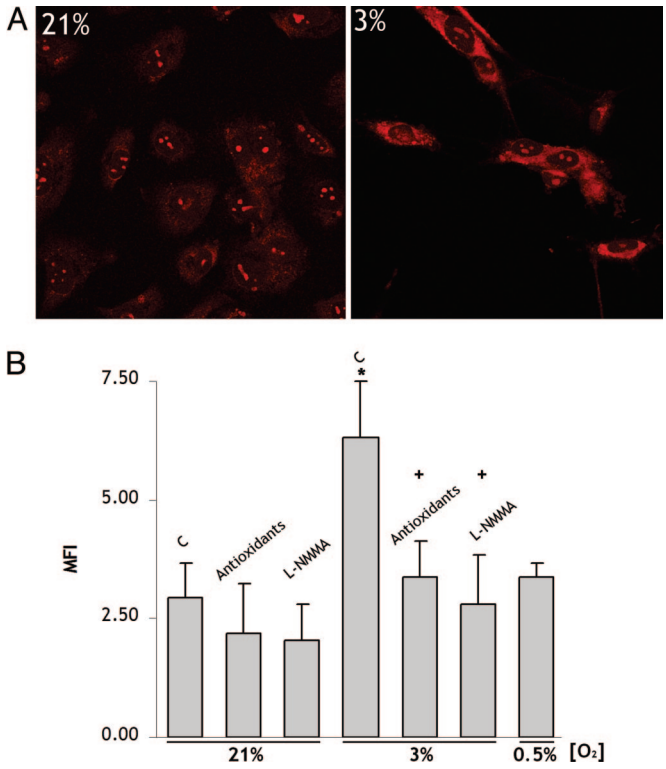

Fig. 2. ROS generation in HUVECs at different O_2 concentrations. (*A*) Representative confocal images of HUVECs exposed to two different O_2 concentrations. (*B*) Fluorescence of DHE oxidation products, as measured by flow cytometry, from intact cells incubated with DHE indicating intracellular superoxide production in the presence or absence of L-NMMA and antioxidants (50 μM MnTBAP plus 1 mM ascorbic acid) at 21%, 3%, and 0.5% O_2. MFI, mean fluorescence intensity. *, Significantly different from control (C) 21% ($P < 0.05$); +, significantly different from control (C) 3% ($P < 0.05$).

HIF-1α stabilization at a very low O_2 concentration, at which the release of ROS is greatly decreased or disappears altogether (21). Nevertheless, evidence for a mitochondrial ROS involvement in HIF-1α stabilization is documented in other systems; therefore, the reasons for the absence of this mechanism in endothelial cells deserve further investigation. One

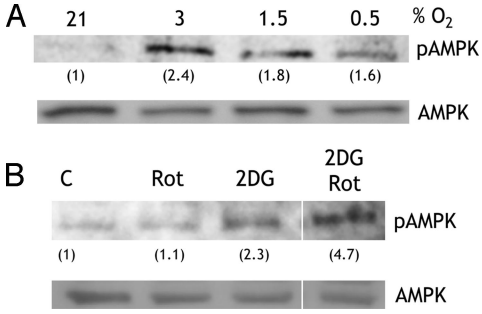

Fig. 3. Effect of O_2 concentration and metabolic inhibitors on AMPK activation in HUVECs. (*A*) HUVECs were incubated for 2 h at different O_2 concentrations (21%, 3%, 1.5%, and <0.5%) in a controlled hypoxic chamber, and AMPK activation was assessed by Western blotting. (*B*) AMPK activation by bioenergetic crisis under normoxic conditions. Phosphorylated AMPK (pAMPK) in HUVECs treated with different glycolytic and mitochondrial inhibitors (20 mM 2DG and 0.5 μM rotenone) was assessed by Western blotting. These are representative data from at least three independent experiments. The values in brackets are the estimations from densitometry analysis. Rot, rotenone; AMPK, loading control.

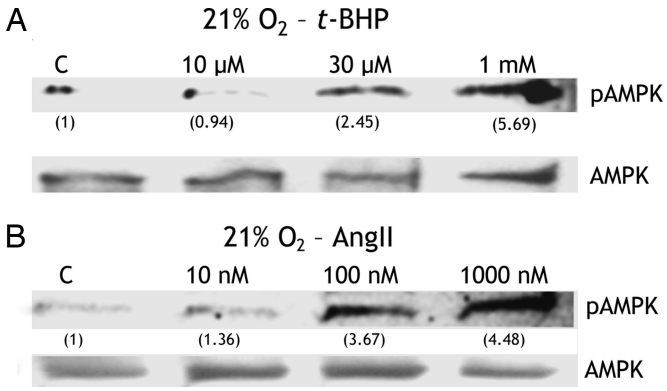

Fig. 4. AMPK activation by ROS. (*A*) HUVECs were treated with the indicated concentrations of *tert*-butylhydroxyperoxide for 2 h under normoxic conditions. (*B*) HUVECs were incubated with the indicated concentrations of angiotensin II for 30 min under normoxic conditions. In both cases, phosphorylated AMPK (pAMPK) was detected by Western blotting as detailed in *Materials and Methods*. Values in brackets are the estimations from densitometry analysis. C, control; AMPK, loading control.

possibility is that HIF-1α stabilization depends on the generation of ROS in conditions more akin to pathophysiology than physiology, as we and others have shown in cancer cells (22, 23). However, even in the absence of NO, HUVECs stabilize HIF-1α at concentrations of O_2 substantially lower than other cells ($\approx$1.5%). A possible explanation for this phenomenon could be the presence of high concentrations of prolyl hydroxylases in endothelial cells (ref. 24 and our own results) and/or their low respiratory rate ($\approx$2 μM/min per 10^6 cells; ref. 6) compared with those from cells such as astrocytes and neurons (more than $\approx$5 μM/min per 10^6 cells; ref. 25). A low O_2 consumption might spare O_2, thus enabling prolyl hydroxylases to function at a lower O_2 concentration than normal (7, 26).

As demonstrated before (27–29), endothelial cells are highly glycolytic. We have shown that, even at very low O_2 concentrations, HUVECs maintain an unchanged [ATP] during the period of observation (2 h). ATP concentrations could be significantly affected only by interfering with glucose metabolism. Thus, energy production in HUVECs is mainly from glycolysis, a feature shared with cancer cells (30), despite the fact that HUVECs have functional and active mitochondria able to use other substrates such as glutamine and palmitate, especially in situations in which glucose is low (27) or when fatty acids are increased (31). Therefore, our results suggest that mitochondria in HUVECs are not preferentially used for bioenergetic purposes; instead, under the control of NO, they seem to be acting as signaling organelles. Indeed, at a significantly higher O_2 concentration than that at which HIF-1α is stabilized, AMPK is activated through a mechanism that is mitochondria-dependent but independent of changes in nucleotide levels.

Since its discovery, AMPK has been suggested to serve as an energy gauge in cells, detecting changes in the AMP:ATP ratio (32). The consequences of AMPK activation include inhibition of acetyl CoA carboxylase and fatty acid synthesis, activation of 6-phosphofructo-2-kinase and glycolysis, β-oxidation promotion, and, as recently claimed, modulation of gene expression (33, 34). Recently, however, activation of the enzyme by mechanisms independent of the AMP:ATP ratio has been described (35, 36), including a ROS-mediated mechanism (37–39).

Our experiments indicate that AMPK activation in HUVECs at low O_2 concentrations depends on mitochondrial ROS generation because (*i*) it coincides with the O_2 concentration at which maximum release of ROS is observed, (*ii*) the use of antioxidants prevents AMPK activation, and (*iii*) it does not occur in ρ^0 HUVECs devoid of functional mitochondria. A ROS-mediated mechanism for AMPK activation is further supported by our experiments using a prooxidant such as *tert*-butylhydroxyperoxide or angiotensin II, as others have previously demonstrated (40).

The activation of AMPK by a ROS-dependent mechanism is intriguing and might indicate a role in cellular defense. Indeed, a protective role for AMPK activation in endothelial cells has recently been suggested related to cardioprotection and the inactivation of caspase-3 (41, 42). It is not known whether other protective mechanisms are also activated. Release of ROS has been shown to contribute to the activation of other transduction mechanisms involved in cellular defense such as NF-κB (43), AP1 (44), and p53 (45). It has also been claimed to mediate pharmacological responses such as pulmonary vasoconstriction to hypoxia (46) and cold-induced constriction of cutaneous arteries (47). Our present and previous experiments (6) suggest that this is not a response to hypoxia *per se* because it takes place at O_2 concentrations higher than those that would be considered hypoxic. Moreover, the release of ROS occurs in the absence of significant changes in O_2 consumption and in endothelial cells which, because of their glycolytic nature, are able to preserve their bioenergetic status under hypoxic conditions. It is more likely that, as we have suggested, this release of ROS is an early stress response dependent primarily on the mitochondrial redox status, and it is modulated by NO (6).

Interestingly, the catalytic AMPK-α1 subunit is the only one present in endothelial cells (our unpublished observations). This distribution is unlike liver, cardiomyocytes, and skeletal muscle (48), where both catalytic subunits (α1 and α2) are expressed. Although there is clear evidence for the activation of the α2-subunit of AMPK being dependent on bioenergetic crisis (49), the α1-subunit is known to be far less responsive to changes in AMP. Our experiments are in agreement with this observation, because very substantial changes in the AMP:ATP ratio were required for us to observe activation of AMPK in HUVECs. Whether there are differences between the downstream mechanisms activated by each of the catalytic subunits is not known at present.

In conclusion, our results indicate that in vascular endothelial cells mitochondria prevent the stabilization of HIF-1α and generate ROS for activation of AMPK. We suggest that these two actions, which are NO-dependent, are important for the maintenance of the nonangiogenic and highly resistant phenotype of endothelial cells. Whether mitochondria also play a key role in diverting O_2 from the

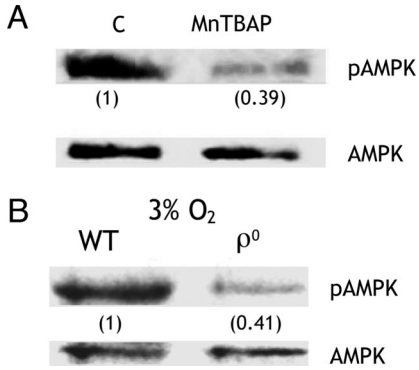

Fig. 5. Control of AMPK activation at 3% O_2. AMPK phosphorylation was assessed by Western blotting after different treatments. (*A*) HUVECs were incubated for 2 h in the absence (C) or presence of a SOD mimetic (50 μM MnTBAP). (*B*) ρ^0 cells lacking functional mitochondria were incubated at 3% O_2 for 2 h. Representative results from at least three independent experiments are presented. Values in brackets are the estimations from densitometry analysis. C, control; AMPK, loading control.

glycolytic endothelium to the O_2-requiring vascular smooth muscle needs further investigation.

Materials and Methods

Cells and Reagents. HUVECs were purchased from PromoCell (Heidelberg, Germany). Cells were grown until passage 3–5 in endothelial cell growth medium (EGM 2, PromoCell) at 37°C in a 5% CO_2/humidified air incubator. All experimental procedures were carried out when the cells were 80% confluent. ρ^0 endothelial cells were prepared essentially as described by King and Attardi (50). Briefly, after 3 weeks of treatment with ethidium bromide, the lack of mitochondrial function was verified by the absence of expression of two intrinsic mitochondrial genes using RT-PCR [cytochrome oxidase subunit 1 (GenBank accession no. AF381998), 5′-ATTTAGCTGACTCGCCACACTCCA-3′ and 5′-TAGGCCGAGAAAGTGTTGTGGGAA-3′; and ATPase subunit 6 (GenBank accession no. AY963585), 5′-ACATTACTGCAGGCCACCTACTCA-3′ and 5′-ACGTAGGCTTGGATTAAGGCGACA-3′]. Smooth muscle cells from corpus cavernosum were provided by S. Cellek (GlaxoSmithKline, Harlow, Essex, U.K.). Human epithelial kidney cells (HEK293) were purchased from Invitrogen. Hypoxia was achieved by incubation of the cells at 37°C in an O_2-controlled hypoxic chamber (Coy Laboratory Products, Ann Arbor, MI) for 2–8 h. *N*-acetyl-L-cysteine, L-ascorbic acid, 2DG, antimycin A, myxothiazol, *tert*-butylhydroperoxide, angiotensin II, and rotenone were purchased from Sigma; L-NMMA was purchased from Alexis (Nottingham, U.K.). Anti-eNOS antibodies were obtained from Santa Cruz Biotechnology, and anti-phospho-AMPK-α_1-Thr-172 and anti-AMPK antibodies were from Cell Signaling Technology (Beverly, MA) and used as indicated by the supplier.

eNOS Silencing. HUVECs were infected with pSIN-sh eNOS-Puro, a self-inactivating lentiviral vector expressing a short-hairpin RNA molecule against eNOS (GenBank accession no. NM_000603) by using the following oligos: 5′-TTCATCAACCAGTACTACAGCttcgGCTGTAGTACTGGTTGATGAAGttttt-3′ and 5′-ctagAAAAACTTCATCAACCAGTACTACAGCcgaaGCTGTAGTACTGGTTGATGAA-3′ (MWG Biotech). These oligos were annealed in Mg^{2+}-free PCR buffer (Promega) for 2 min at 95°C and allowed to cool slowly to room temperature using a water bath. The resulting mixture was inserted into pGEM-U6L (a gift from Sam Wilson, Windeyer Institute, University College London) cut with SalI (blunted with mung bean nuclease; Promega) and XbaI. The cassette carrying the interference RNA (iRNA) structure was subcloned into pSIN-Puro (a gift from Greg Towers, Windeyer Institute, University College London) using EcoRI. The insert orientation was found not to affect the silencing ability. This plasmid was then used to create lentiviral vectors as previously described by Ikeda *et al.* (51). All constructs were verified by DNA sequencing.

Western Blot Analysis. HUVECs were grown for 1 week, with a change of medium every 2 days. On the day of the experiment, fresh medium was added and treatments were performed as indicated. Cells were washed with PBS, scraped off in ice-cold PhosphoSafe buffer (Novagen), and centrifuged for 10 min at 13,000 × *g* (4°C). From clear supernatants, protein concentration was determined by the DC Bio-Rad kit using BSA as control. Sample aliquots were boiled for 2 min, and equal amounts (usually 20 μg) of total protein were electrophoresed in precast SDS/PAGE 4–15% gradient gels (Bio-Rad). Proteins were transferred to nitrocellulose membranes (Amersham Pharmacia), assessed for equal loading/transference by Red Ponceau tinction, and immunoblotted overnight with the indicated primary antibodies (typically 1:1,000 dilution) followed by secondary antibody conjugated with horseradish peroxidase (1:5,000 dilution). The ECL Plus Western blotting detection kit (Amersham Pharmacia Biosciences) was used for detection.

Accumulation and Activation of HIF-1α. HUVECs were incubated for 8 h under different treatments. Nuclear extraction was carried out as described in ref. 6. Protein content in the nuclear extracts was determined to adjust the amount to 60 μg per well for each sample. Samples were analyzed by Western blotting using a mouse monoclonal antibody (BD Biosciences) against HIF-1α (1:2,500), followed by an anti-mouse horseradish peroxidase conjugate (1:2,500; DAKO) and enhanced chemiluminescence (Amersham Pharmacia). HIF-1α activation was quantified in 5–10 μg of nuclear extracts by specific binding of HIF-1α to the hypoxia response element, a 5′-RCGTG-3′ consensus sequence, using the TransAM HIF-1 Kit (Active Motive, Reixensart, Belgium) according to the manufacturer's instructions.

Intracellular Superoxide Production. HUVECs were incubated with 10 μM DHE in the absence or presence of different treatments. After 1-h exposure to different O_2 concentrations, cells were washed with PBS or with 3% O_2-equilibrated PBS, respectively, to remove excess DHE. Cells were fixed for 10 seconds with 0.5 ml of 70% ethanol on ice and were then resuspended in 1 ml of normal PBS and analyzed immediately by flow cytometry (FACSCalibur, Becton Dickinson). Data were acquired and analyzed using CELLQUEST software. Results are expressed as the mean fluorescence intensity.

Determination of Adenine Nucleotides. For experiments involving ATP determination HUVECs were grown for 24 h in 96-well plates (PerkinElmer 3603 clear bottom, black walls, seeding density 5,000 cells per well) in a phenol red-free medium. On the day of the experiment, fresh medium was added and treatments were performed as indicated. ATP was measured by the luciferin/luciferase method with a chemiluminescence kit (PerkinElmer) following the manufacturer's protocol. Chemiluminescence was determined in a TopCount (Packard Biosciences), and data were analyzed in EXCEL (Microsoft). Alternatively, for simultaneous determination of AMP and ATP, HUVECs were grown for 24 h on six-well plates (3×10^5 cells per well). After treatments, nucleotides were extracted, separated by HPLC, and quantified as described by Smolenski *et al.* (52).

Statistics. Values stated are means ± SEM. To compare data obtained under different conditions an ANOVA test was used. Results were considered to be significantly different when $P < 0.05$.

We thank Annie Higgs and Jorge Erusalimsky for their critical reading of this article. M.Q. [formerly a Ph.D. student at the University of Valencia (Valencia, Spain)] is the recipient of a fellowship from the Ministerio de Sanidad y Consumo of Spain. S.L.C. is sponsored by a grant from the Wellcome Trust. S.M. is the recipient of a grant from the Medical Research Council.

1. Moncada, S., Palmer, R. M. J. & Higgs, E. A. (1991) *Pharmacol. Rev.* **43,** 109–142.
2. Cleeter, M. W. J., Cooper, J. M., Darley-Usmar, V. M., Moncada, S. & Schapira, A. H. V. (1994) *FEBS Lett.* **345,** 50–54.
3. Brown, G. C. & Cooper, C. E. (1994) *FEBS Lett.* **356,** 295–298.
4. Schweizer, M. & Richter, C. (1994) *Biochem. Biophys. Res. Commun.* **204,** 169–175.
5. Moncada, S. & Erusalimsky, J. D. (2002) *Nat. Rev. Mol. Cell Biol.* **3,** 214–220.
6. Palacios-Callender, M., Quintero, M., Hollis, V. S., Springett, R. J. & Moncada, S. (2004) *Proc. Natl. Acad. Sci. USA* **101,** 7630–7635.
7. Hagen, T., Taylor, C. T., Lam, F. & Moncada, S. (2003) *Science* **302,** 1975–1978.
8. Almeida, A., Moncada, S. & Bolanos, J. P. (2004) *Nat. Cell Biol.* **6,** 45–51.

9. Clementi, E., Brown, G. C., Foxwell, N. & Moncada, S. (1999) *Proc. Natl. Acad. Sci. USA* **96,** 1559–1562.
10. Mann, G. E., Yudilevich, D. L. & Sobrevia, L. (2003) *Physiol. Rev.* **83,** 183–252.
11. Wang, G. L., Jiang, B. H., Rue, E. A. & Semenza, G. L. (1995) *Proc. Natl. Acad. Sci. USA* **92,** 5510–5514.
12. Sutter, C. H., Laughner, E. & Semenza, G. L. (2000) *Proc. Natl. Acad. Sci. USA* **97,** 4748–4753.
13. Jiang, B. H., Rue, E., Wang, G. L., Roe, R. & Semenza, G. L. (1996) *J. Biol. Chem.* **271,** 17771–17778.
14. Hardie, D. G., Carling, D. & Carlson, M. (1998) *Annu. Rev. Biochem.* **67,** 821–855.
15. Carling, D. (2004) *Trends Biochem. Sci.* **29,** 18–24.
16. Uruno, A., Sugawara, A., Kanatsuka, H., Kagechika, H., Saito, A., Sato, K., Kudo, M., Takeuchi, K. & Ito, S. (2005) *Circulation* **112,** 727–736.
17. Griendling, K. K., Minieri, C. A., Ollerenshaw, J. D. & Alexander, R. W. (1994) *Circ. Res.* **74,** 1141–1148.
18. Tang, N., Wang, L. C., Esko, J., Giordano, F. J., Huang, Y., Gerber, H. P., Ferrara, N. & Johnson, R. S. (2004) *Cancer Cell* **6,** 485–495.
19. Manalo, D. J., Rowan, A., Lavoie, T., Natarajan, L., Kelly, B. D., Ye, S. Q., Garcia, J. G. N. & Semenza, G. L. (2005) *Blood* **105,** 659–669.
20. Chandel, N. S., Maltepe, E., Goldwasser, E., Mathieu, C. E., Simon, M. C. & Schumacker, P. T. (1998) *Proc. Natl. Acad. Sci. USA* **95,** 11715–11720.
21. Schroedl, C., McClintock, D. S., Budinger, G. R. S. & Chandel, N. S. (2002) *Am. J. Physiol.* **283,** L922–L931.
22. Quintero, M., Brennan, P. A., Thomas, G. J. & Moncada, S. (2006) *Cancer Res.* **65,** 5512–5515.
23. Gerald, D., Berra, E., Frapart, Y. M., Chan, D. A., Giaccia, A. J., Mansuy, D., Pouyssegur, J., Yaniv, M. & Mechta-Grigoriou, F. (2004) *Cell* **118,** 781–794.
24. Cioffi, C. L., Liu, X. Q., Kosinski, P. A., Garay, M. & Bowen, B. R. (2003) *Biochem. Biophys. Res. Commun.* **303,** 947–953.
25. Almeida, A., Almeida, J., Bolanos, J. P. & Moncada, S. (2001) *Proc. Natl. Acad. Sci. USA* **98,** 15294–15299.
26. Doege, K., Heine, S., Jensen, I., Jelkmann, W. & Metzen, E. (2005) *Blood* **106,** 2311–2317.
27. Culic, O., Gruwel, M. L. H. & Schrader, J. (1997) *Am. J. Physiol.* **273,** C205–C213.
28. Mertens, S., Noll, T., Spahr, R., Krutzfeldt, A. & Piper, H. M. (1990) *Am. J. Physiol.* **258,** H689–H694.
29. Tretyakov, A. V. & Farber, H. W. (1995) *J. Clin. Invest.* **95,** 738–744.
30. Gatenby, R. A. & Gillies, R. J. (2004) *Nat. Rev. Cancer* **4,** 891–899.
31. Dagher, Z., Ruderman, N., Tornheim, K. & Ido, Y. (2001) *Circ. Res.* **88,** 1276–1282.
32. Hardie, D. G. & Carling, D. (1997) *Eur. J. Biochem.* **246,** 259–273.
33. Young, L. H., Li, J., Baron, S. J. & Russell, R. R. (2005) *Trends Cardiovasc. Med.* **15,** 110–118.
34. Leff, T. (2003) *Biochem. Soc. Trans.* **31,** 224–227.
35. Woods, A., Dickerson, K., Heath, R., Hong, S. P., Momcilovic, M., Johnstone, S. R., Carlson, M. & Carling, D. (2005) *Cell Metab.* **2,** 21–33.
36. Hawley, S. A., Pan, D. A., Mustard, K. J., Ross, L., Bain, J., Edelman, A. M., Frenguelli, B. G. & Hardie, D. G. (2005) *Cell Metab.* **2,** 9–19.
37. Zou, M. H., Hou, X. Y., Shi, C. M., Kirkpatrick, S., Liu, F., Goldman, M. H. & Cohen, R. A. (2003) *J. Biol. Chem.* **278,** 34003–34010.
38. Zou, M. H., Kirkpatrick, S. S., Davis, B. J., Nelson, J. S., Wiles, W. G., Schlattner, U., Neumann, D., Brownlee, M., Freeman, M. B. & Goldman, M. H. (2004) *J. Biol. Chem.* **279,** 43940–43951.
39. Toyoda, T., Hayashi, T., Miyamoto, L., Yonemitsu, S., Nakano, M., Tanaka, S., Ebihara, K., Masuzaki, H., Hosoda, K., Inoue, G., *et al.* (2004) *Am. J. Physiol.* **287,** E166–E173.
40. Nagata, D., Takeda, R., Sata, M., Satonaka, H., Suzuki, E., Nagano, T. & Hirata, Y. (2004) *Circulation* **110,** 444–451.
41. Ido, Y., Carling, D. & Ruderman, N. (2002) *Diabetes* **51,** 159–167.
42. Russell, R. R., Li, J., Coven, D. L., Pypaert, M., Zechner, C., Palmeri, M., Giordano, F. J., Mu, J., Birnbaum, M. J. & Young, L. H. (2004) *J. Clin. Invest.* **114,** 495–503.
43. Pahl, H. L. & Baeuerle, P. A. (1994) *BioEssays* **16,** 497–502.
44. Millhorn, D. E., Raymond, R., Conforti, L., Zhu, W., Beitner-Johnson, D., Filisko, T., Genter, M. B., Kobayashi, S. & Peng, M. (1997) *Kidney Int.* **51,** 527–535.
45. Achison, M. & Hupp, T. R. (2003) *Oncogene* **22,** 3431–3440.
46. Waypa, G. B. & Schumacker, P. T. (2005) *J. Appl. Physiol.* **98,** 404–414.
47. Bailey, S. R., Mitra, S., Flavahan, S. & Flavahan, N. A. (2005) *Am. J. Physiol.* **289,** H243–H250.
48. Cheung, P. C. F., Salt, I. P., Davies, S. P., Hardie, D. G. & Carling, D. (2000) *Biochem. J.* **346,** 659–669.
49. Salt, I., Celler, J. W., Hawley, S. A., Prescott, A., Woods, A., Carling, D. & Hardie, D. G. (1998) *Biochem. J.* **334,** 177–187.
50. King, M. P. & Attardi, G. (1989) *Science* **246,** 500–503.
51. Ikeda, Y., Collins, M. K. L., Radcliffe, P. A., Mitrophanous, K. A. & Takeuchi, Y. (2002) *Gene Ther.* **9,** 932–938.
52. Smolenski, R. T., Lachno, D. R., Ledingham, S. J. M. & Yacoub, M. H. (1990) *J. Chromatogr. Biomed. Appl.* **527,** 414–420.